

RADIOMETRIC MONITORING OF ATMOSPHERIC BOUNDARY LAYER TEMPERATURE PROFILES

B. R. Westwater*, A. S. Vyazankin**, K. P. Gaikovich**,
E. N. Kadyrov**, and D. Yu. Moiseev**

A statistical analysis is presented of intercomparison results of simultaneous measurements of atmospheric boundary layer temperature profiles using three independent methods: radiometric, radioacoustic, and in situ. The data allowed the evaluation of the mean square error of each of the methods individually and the optimization of the algorithm for retrieving temperature profiles from radiometric data by minimizing the mean square error.

I. INTRODUCTION

One of the current problems of the development of contemporary methods and technological means of obtaining meteorological information is the creation of remote-sensing methods and instruments for measuring atmospheric temperature profiles. In particular, one of these methods is radiometric based on the measurements of thermal emission or the atmosphere in the millimeter wavelength band with a subsequent reconstruction of temperature profiles from the radiometric data. The radiometric method of reconstruction of the temperature profiles from thermal emission measurements at frequencies in the absorption band of molecular oxygen with a center at 60 GHz was developed for more than three decades beginning with the works [6-10, 12, 15, 16], where measurements on the wings of this band were used to reconstruct profiles up to heights of few kilometers. In above works, the primary method used the statistical dependence between satellite measurements and meteorological observations to solve the problem of regularization that arises in ill-posed inverse problems that are reduced to Fredholm integral equations of the first kind.

In [2, 4, 11], it was shown that such an approach does not take into account boundary-layer characteristics both from the point of view of the information content of the measurements and from the point of view of the solution of the inverse problem. For measurements on the slope of the frequency spectra of oxygen, temperature variations at differed heights of the atmospheric boundary layer lead to insignificant increases in the radio brightness temperature (as a rule, this is one hundredth or one thousandth of a degree). On the other hand, statistical method for solving the inverse problem do not take into account the characteristics of the boundary layer that are associated with strong temperature changes at various heights in the boundary layer.

To solve the problems stated above, in [4] it was proposed, first, to use angular observations at frequencies close to the maximum of the oxygen band (60 GHz) to measure radiation that is emitted inside the boundary layer; secondly, a method for solving the inverse problem was developed, based the rigorous theory of ill-posed problems of Tikhonov, which takes into account the specific characteristics of

* National Atmospheric and Oceans Administration, Boulder, USA

** Central Aerological Observatory

the inverse problem in [2, 11] this method was successfully applied for retrieval of the temperature profile from angular measurements with the help of a specially developed radiometer. The high sensitivity of this wide-band radiometer, the low level of influence of side lobes, the minimum error level, and a calibration method based on the creation of a large contrast in temperature between calibration standards, one of which was the temperature of the near-surface layer, lead to a measurement accuracy of 0.05 K. This accuracy is necessary for the effective reconstruction of the majority of types of vertical temperature distribution in the boundary layer, even elevated inversions. Comparison with direct measurements confirmed the accuracy of the method.

The vertical resolution of the latter method essentially depends on the width of the directional diagram of the radiometer antenna. In particular, the radiometer (width of the directions diagram is θ), used in the comparison described further, has a vertical resolution of 50 m up to a height of 300 m and is of the order of 100 m at heights of 300-600 m.

In the given work, results are given of an experiment of the field variations of a radiometer that is capable of working automatically during a sufficiently infrequent and simplified procedure of automatic calibration.

From November 1996 to March 1997 at the Boulder Atmospheric Observatory (USA) a comparison was made between several methods of measurement of temperature profiles of the atmospheric planetary boundary layer (PBL) [13, 14]. In these investigations, remote and in situ instruments of the National Oceanic and Atmospheric Administration (NOAA, USA) were used; a radioacoustic sounder, in situ sensors placed on a meteorological tower, radiosondes, and also a Russian scanning radiometer in the millimeter wavelength region (MTP-5). The in situ sensors were placed on the 100-m high meteorological tower at the levels of 10, 50, 100, 200, and 300 m. These were platinum resistance thermometers with a nominal temperature measurement accuracy of 0.2 K, with data being recorded every 15 minutes. The radioacoustic sounding system (RASS; operated at the frequency of 915 MHz, in the height interval from 100 to 615 m with a vertical resolution of 60 m and a nominal accuracy of 1.0 K. The information from the RASS was available every hour; however, it should be noted that the radioacoustic data were not sufficiently reliable for all meteorological conditions; therefore, only about 20% of these data were used for our comparisons. The Russian scanning radiometer MTP-5 had the following basic characteristics: center frequency 59.8 GHz; total bandwidth 4 GHz, sensitivity 0.04 K for an integration time of 1 s; scanning step 9° ; frequency of measurement 5 min [11, 14]. The radiometric data were reliable for all meteorological conditions; during the entire time of comparisons, there was no case when the radiometric data were missing. The first results of the comparisons showed a high degree of similarity between data that were obtained by different methods [13, 14]. A high degree of reliability and accuracy of the original information (100 temperature profiles obtained by three methods simultaneously and 2000 profiles by the radiometric method and from measurements on the meteorological tower) allows a detailed analysis of the retrieval accuracy of planetary boundary layer temperature profiles confirmed by comparison with results of other independent temperature measurements.

The most important feature of the analysis of the retrieval accuracy of temperature profiles is the fact that statistical analysis of difference characteristics allows the evaluation of the standard deviation of each of the three methods separately) - from the true temperature profile. Analogous to analysis of the three statistical ensembles, it is possible, by solving the direct problem, i.e., by calculating the radio brightness temperature from the data of the other two methods and then comparing these calculations with the data from the scanning radiometer, to obtain a realistic evaluation of the mean square error of the measurements of the MTP-5 radiometer. Finally, this allows the optimization of the method for retrieving temperature profiles to obtain the minimum mean square error of reconstruction.

2. METHOD OF RETRIEVAL OF TEMPERATURE PROFILES

Retrieval of the temperature profile is based on the solution of the equation that relates temperature profile $T(h)$ with the brightness temperature of the thermal emission of the atmosphere T_B measured at the frequency of 60 GHz as a function of the angle θ :

$$T_B(\theta) = \int_0^\infty T(h)K(h,\theta)dh \cong \frac{1}{\cos\theta} \int_0^\infty T(h) \gamma e^{-\gamma h/\cos\theta} dh \tag{1}$$

where K is the equation kernel and γ the absorption coefficient at 60 GHz. The evaluations [2,6,11] show that we can neglect the dependence of γ on temperature and pressure within the atmospheric boundary layer. Then the equation assumes a simple form represented by the right-hand side of (1). Nevertheless, in the first approximation, the algorithm of solution takes into account this dependence and, as needed, permits an iterative procedure for solution of nonlinear equations, which, as has been shown is not necessary.

By considering the width of the directional diagram of the scanning radiometer (6°), an algorithm was developed to take into account the difference between antenna and brightness temperatures. The antenna temperature is represented as the convolution, with respect to angle, of the brightness temperature with the antenna pattern

$$T_B(\theta_0) = \int_{-\infty}^\infty \Phi(\theta - \theta_0)d\theta \int_0^\infty T(h)K(h,\theta)dh = \int_0^\infty T(h)dh \int_0^\infty \Phi(\theta - \theta_0)K(h,\theta)d\theta \tag{2}$$

The latter integral on the right-hand side of Eq. (2) forms a new kernel K' in the equation for the antenna temperature, which is also an equation with constant limits of the type of Fredholm equation of the first kind.

$$T_A(\theta_0) = \int_0^\infty T(h)K'(h,\theta_0)dh \tag{3}$$

We now consider methods of solving the equation.

Tikhonov's Method

The basic approach to solving (3) as well as Eq. (1) in [2, 4, 11], was based on the application of Tikhonov's principle of the generalized residual (see [5], p. 101) which uses largely general information on the quadratic summation of the exact solution and its derivative. The principle solves the problem for the class of continuous functions and corresponds well with the characteristics of the problem under consideration.

We transform (3) into operator form

$$\mathbf{K}'T = T_B^\delta \tag{4}$$

where T_B is a vector or data obtained with some error, the measure of which in Tikhonov's method is the integrated error δT_B , defined as

$$\delta T_B^2 = \left\| \mathbf{K}'T - T_B^\delta \right\|_{L_2}^2 = \frac{1}{\theta_0^{\max}} \int_0^{\theta_0^{\max}} [T_B(\theta_0) - T_B^\delta(\theta_0)]^2 d\theta_0 \tag{5}$$

where T_B is the right-hand side of (4), which corresponds to the exact solution $T(h)$, $\|x\|_{L_2}^2$ is the norm of the function x in the space L_2 , [5], and θ_0^{\max} is the maximum value of θ_0 , which, in the given case, is close to $\pi/2$.

In Tikhonov's method [5], the approximate solution minimizes the smoothing functional

$$M^\alpha(T) = \left\| \mathbf{K}T - T_B^\delta \right\|_{L_2}^2 + \alpha \|T\|_{W_2^1}^2, \tag{6}$$

i.e. by minimizing the functional, it is possible to find the solution. In the relations mentioned above

$$\|T\|_{W_2^1}^2 = \frac{1}{h^{\max}} \int_0^{h^{\max}} [T(h)^2 + (h^{\max} \frac{dT(h)}{dh})^2] dh$$

designates the norm of the function $T(h)$ as an element of the functional space W_2^1 [5], and h^{\max} is the height of the upper boundary layer in which the solution is sought. The problem of minimization of a convex functional, such as (6), after she corresponding discretization leads to its well-studied finite-dimensional analog. This problem, from a calculational point of view, is a problem of quadratic programming, and can be solved by standard gradient methods. In the present work, the method of conjugate gradients is applied, which is described, for example, in [1] (in [5], its algorithm is given in FORTRAN). The numerical realization of the method, which in the present work is written in Borland Pascal 7.0, solves the problem in 0.5 s on an IBM-Penium-200 PC.

The regularization parameter α in the second term of (6) determines the degree of smoothness of the approximate equation, it is precisely this stabilizing term that ensures convexity, and consequently, the possibility of minimization of the functional and solution of the equation, The solution obtained is selected from the set of functions that satisfy the original ill-posed equation, and is minimal in the sense of the norm of the stabilizing term W_2^1 that contains the function itself and its derivative, i.e. a condition is realized of some compromise between minimization in absolute value and smoothness of the original function. As shown in [5], the regularization parameter α is uniquely connected with the integral measure of the data error (by a number) and diminishes with decreasing level of error, but more slowly. This is a large advantage of the method of the generalized residual. In addition, with increasing accuracy the role of the second stabilizing term in (6) gradually decreases. The parameter α is found as a root of the one-dimensional nonlinear equation of the generalized residual

$$\rho(\alpha) = \left\| \mathbf{K}'T^\alpha - T_B^\delta \right\|_{L_2}^2 - \delta^2 = 0, \tag{7}$$

where T^α is the function that minimizes functional (6), i.e., the algebraic equation (7) is solved simultaneously with the functional equation (6). The meaning of (7) is that the norm of the residual of the solution obtained must be as accurate as the norm of the error, since there is no reason to minimize the departure from the measured data beyond the limits of the error level. The parameter of the effective error δ enters into Eq. (7) and must be determined a priori from the specific conditions of the solution of the problem. This parameter must include all components of measurement and interpretation errors. In particular, δ must include the measurement error δT_B , both random and systematic components, and also the error in the kernel δ_h , which includes the error of discretization for numerical solution and the possibility of inaccuracy in the approximation of the corresponding functions

$$\delta^2 = \left\| \mathbf{K}_h T - T_B^\delta \right\|_{L_2}^2 \leq (\delta T_B + \delta_h)^2 \tag{8}$$

In Tikhonov's method, the values of the parameters entering into (8) must represent the corresponding maximal estimates in the class of possible realizations of the original function The parameter α , and consequently, the degree of smoothness of the solution, is connected with the effective error parameter δ .
The

latter circumstance is one of the main merits of the method, since the investigator's subjectivity is carried over from the realm of interpretation of experimental data to the evaluation of the error of real measurements. Since the error always contains some uncertainty, there is a possibility of choosing a strategy of solution. Thus, if the problem is posed of automatically excluding nonexistent details in the solution, it is better to accept the error estimate with some excess, which, of course, can lead to the smoothing of some real line-structure details. If in solving the problem it is more important to present and not to miss these details, then one must accept the least error from a region of its possible values. In this case, however, the appearance in the solution of really nonexistent (false) details becomes possible. A proper evaluation of the errors gives the optimal solution in the sense of Tikhonov's method. After determination of δ , the procedure of obtaining the final results becomes formal.

A very important advantage of the method of the generalized residual in comparison with other well-known methods is that as δ tends to zero in the integral metric (i.e., in the metric where the norm is the maximum modulus), the approximate solution converges uniformly to the exact one, although as a rule, in contrast to well-posed problems, the speed of convergence is not proportional to a decrease in δ , but slower. To evaluate the errors, the uniform convergence allows the use of elementary numerical experiments with typical or extremal initial distributions. These experiments are impossible to do in cases that have integral or mean-quadratic convergence.

The parameter δ_h is determined from numerical modeling, and the problem of creating an effective algorithm is its minimization to a level that is negligibly small in comparison with measurement errors. Tikhonov's method [5] also examines the role of possible inconsistencies on the right-hand side of equations of the type (3), which leads to some additional contribution to the effective error. The contribution does not exceed the level of measurement error. In the present work, since the effective error is nonetheless the parameter that we seek to minimize the mean square retrieval error over the ensemble of data, we do not dwell on the introduction of this component.

The numerical modeling shows that significant improvement in the accuracy of reconstruction can be obtained if the equation is solved, as the departure from a sufficiently close first approximation to an exact solution, which must belong to a class of functions in which the solution is sought. In this case, the right-hand side of Eq. (3) represents the departures of measurements of brightness temperature from calculations that use the first approximation.

The Exact Solution for a Linear Profile

There exist simplified approaches to the solution of equations of the type (3) that are based on the application of various approximations of the solution by well-known functions, on the use of series expansion in powers of the arguments or in eigenfunctions of the kernel bounded by a few of the first terms. The simplest method of reconstruction of the temperature profile is to use the exact solution of (1) for a linear temperature profile

$$T(h) = T_0 + \frac{dT}{dh}h \quad (9)$$

In this case the solution is written, according to [3], as

$$T(h) = T_B(h_{\text{eff}} = h), \quad h_{\text{eff}} = \frac{\cos\theta}{\gamma}, \quad (10)$$

where h_{eff} is the effective thickness of the layer where, at the given angle, the thermal emission is basically formed (skin layer thickness). It is seen that the linear profile is the eigenfunction of the kernel of (1). The application of (10) to the solution of the problem can be justified by the fact that a typical temperature distribution in the troposphere is usually close to linear.

The Exact Solution for a Quadratic Profile

It is possible to advance still farther in the expansion of the solution in powers of height and to obtain an exact solution for a quadratic profile

$$T(h) = T_0 + \frac{dT}{dh}h + \frac{1}{2} \frac{d^2T}{dh^2}h^2 \quad (11)$$

in the form

$$T(h = h_{eff}) = T_B(h_{eff}) + \frac{1}{4} \frac{d^2T_B}{dh_{eff}^2}(h_{eff})h_{eff}^2 \quad (12)$$

From (12) it is seen that the exact solution for a linear profile (10) is partially correct beyond the limits of its applicability, since it enters as the first term into (12), but the term containing the first derivative is missing in (12); and the series continues with the term that contains the second derivative. The solution for a quadratic profile graphically illustrates the incorrectness of the inverse problem, which requires the calculation of the second derivative from experimental data.

3. RESULTS OF STATISTICAL ANALYSIS

The methods described in the previous section were used for the reconstruction of profiles and the subsequent statistical analysis based on three ensembles (number of measurements $N = 100$) of vertical temperature profiles: measured by sensors on the meteorological tower T_{tw} , by the radioacoustic sounder (T_{RASS}) radiometric data (T_R), and also three ensembles of brightness temperature: calculated from temperature profiles, measured by sensors on the meteorological tower ($T_{B,tw}$) and by the sounder ($T_{B,RASS}$), and measured by the scanning radiometer ($T_{B,R}$). For calculations of the brightness temperature which is especially essential at high zenith angles, data from the meteorological tower and the sounder were supplemented by a linearly decreasing temperature profile with a standard gradient of 6.5 K/km, which corresponded to the largest decrease of the calculated brightness temperature from radiometric data.

Each of the three ensembles is characterized by independent errors in the determination of the true temperature (δT_{tw} , δT_{RASS} , and δT_R) or brightness temperature ($\delta T_{B,tw}$, $\delta T_{B,RASS}$, and $\delta T_{B,R}$) as function of height or zenith angle, respectively. Their desired statistical characteristics are the mean values ($\langle \delta T \rangle$, $\langle \delta T_B \rangle$) and dispersions (σT^2 , σT_B^2) and also the average dispersion with respect to zenith angle of the random component of the error of Tikhonov's method (5) δT_B^2 . From the experimental data it is possible to obtain an estimate of the statistical characteristics of the ensemble that is associated with the desired

$$\left\{ \begin{aligned} \Delta T_{B_R-RASS} &= \langle T_{B_R} \rangle - \langle T_{B_{RASS}} \rangle = \langle T_{B_R} - T_{B_{RASS}} \rangle = \langle \delta T_{B_R} - \delta T_{B_{RASS}} \rangle = \langle \delta T_{B_R} \rangle - \langle \delta T_{B_{RASS}} \rangle, \\ \Delta T_{B_R-tw} &= \langle T_{B_R} \rangle - \langle T_{B_{tw}} \rangle = \langle T_{B_R} - T_{B_{tw}} \rangle = \langle \delta T_{B_R} - \delta T_{B_{tw}} \rangle = \langle \delta T_{B_R} \rangle - \langle \delta T_{B_{tw}} \rangle, \\ \Delta T_{B_{RASS}-tw} &= \langle T_{B_{RASS}} \rangle - \langle T_{B_{tw}} \rangle = \langle T_{B_{RASS}} - T_{B_{tw}} \rangle = \langle \delta T_{B_{RASS}} - \delta T_{B_{tw}} \rangle = \langle \delta T_{B_{RASS}} \rangle - \langle \delta T_{B_{tw}} \rangle, \end{aligned} \right. \quad (13)$$

$$\left\{ \begin{aligned} \Delta T_{R-RASS} &= \langle T_R \rangle - \langle T_{RASS} \rangle = \langle T_R - T_{RASS} \rangle = \langle \delta T_R - \delta T_{RASS} \rangle = \langle \delta T_R \rangle - \langle \delta T_{RASS} \rangle, \\ \Delta T_{R-tw} &= \langle T_R \rangle - \langle T_{tw} \rangle = \langle T_R - T_{tw} \rangle = \langle \delta T_R - \delta T_{tw} \rangle = \langle \delta T_R \rangle - \langle \delta T_{tw} \rangle, \\ \Delta T_{RASS-tw} &= \langle T_{RASS} \rangle - \langle T_{tw} \rangle = \langle T_{RASS} - T_{tw} \rangle = \langle \delta T_{RASS} - \delta T_{tw} \rangle = \langle \delta T_{RASS} \rangle - \langle \delta T_{tw} \rangle, \end{aligned} \right. \quad (14)$$

$$\left\{ \begin{aligned} \sigma T_{B_{R-RASS}}^2 &= \left\langle (T_{B_R} - T_{B_{RASS}} - \langle T_{B_R} - T_{B_{RASS}} \rangle)^2 \right\rangle = \sigma T_{B_R}^2 + \sigma T_{B_{RASS}}^2, \\ \sigma T_{B_{R-tw}}^2 &= \left\langle (T_{B_R} - T_{B_{tw}} - \langle T_{B_R} - T_{B_{tw}} \rangle)^2 \right\rangle = \sigma T_{B_R}^2 + \sigma T_{B_{tw}}^2, \\ \sigma T_{B_{RASS-tw}}^2 &= \left\langle (T_{B_{RASS}} - T_{B_{tw}} - \langle T_{B_{RASS}} - T_{B_{tw}} \rangle)^2 \right\rangle = \sigma T_{B_{RASS}}^2 + \sigma T_{B_{tw}}^2, \end{aligned} \right. \quad (15)$$

$$\left\{ \begin{aligned} \sigma T_{R-RASS}^2 &= \left\langle (T_R - T_{RASS} - \langle T_R - T_{RASS} \rangle)^2 \right\rangle = \sigma T_R^2 + \sigma T_{RASS}^2, \\ \sigma T_{R-tw}^2 &= \left\langle (T_R - T_{tw} - \langle T_R - T_{tw} \rangle)^2 \right\rangle = \sigma T_R^2 + \sigma T_{tw}^2, \\ \sigma T_{RASS-tw}^2 &= \left\langle (T_{RASS} - T_{tw} - \langle T_{RASS} - T_{tw} \rangle)^2 \right\rangle = \sigma T_{RASS}^2 + \sigma T_{tw}^2, \end{aligned} \right. \quad (16)$$

The systems of Eqs. (13) and (15) relative to the mean values of the errors are, unfortunately, linearly dependent, and allow one to obtain only estimates of the mean temperature difference, as a function of height for each pair of the three different methods. Taking into account, however, the fact that this dependence (or dependence on zenith angle for brightness temperature) is common to all three methods, it is possible to assume that the absolute maximal difference of the systematic errors will not be worse than the maximal systematic departure of the worst of two pairs of methods. It should also be noted that the elimination of the systematic errors is not as serious problem as the minimization of the random errors.

Dispersions of the random errors can be determined for each of the three methods by solving the system

$$\left\{ \begin{aligned} \sigma T_{B_R}^2 &= \frac{\sigma T_{B_{R-RASS}}^2 + \sigma T_{B_{R-tw}}^2 - \sigma T_{B_{RASS-tw}}^2}{2}, \\ \sigma T_{B_{RASS}}^2 &= \frac{\sigma T_{B_{R-RASS}}^2 - \sigma T_{B_{R-tw}}^2 + \sigma T_{B_{RASS-tw}}^2}{2}, \\ \sigma T_{B_{tw}}^2 &= \frac{-\sigma T_{B_{R-RASS}}^2 + \sigma T_{B_{R-tw}}^2 + \sigma T_{B_{RASS-tw}}^2}{2}, \end{aligned} \right. \quad (17)$$

$$\left\{ \begin{aligned} \sigma T_R^2 &= \frac{\sigma T_{R-RASS}^2 + \sigma T_{R-tw}^2 - \sigma T_{RASS-tw}^2}{2}, \\ \sigma T_{RASS}^2 &= \frac{\sigma T_{R-RASS}^2 - \sigma T_{R-tw}^2 + \sigma T_{RASS-tw}^2}{2}, \\ \sigma T_{tw}^2 &= \frac{-\sigma T_{R-RASS}^2 + \sigma T_{R-tw}^2 + \sigma T_{RASS-tw}^2}{2}, \end{aligned} \right. \quad (18)$$

The dispersion of errors of Tikhonov's method σT_B^2 is determined from (5) by integrating, with respect to zenith angle, the dispersion $\sigma T_{B,R}^2(\theta_0)$ obtained from the first relation of (17).

Figure 1 shows the errors of radiometric measurements. One can see that the level of random errors during continuous measurements in the automatic regime turned out to be higher than the nominal measurement accuracy of 0.04 K. The mean square random component of the error of Tikhonov's method of σT_B , determined from the data presented in Fig. 1, was 0.5 K. The average departures of the measured brightness temperatures from those calculated using temperature profiles measured on the meteorological tower turned out to be small in comparison with the random errors. For the RASS data, the systematic departure is larger, which is caused by, as will be shown below, poor data quality. Figure 2 shows the histogram of the probability density of the distribution of errors of Tikhonov's method in 0.1 K intervals. This histogram assumes that temperature profiles from the RASS (2) or from the meteorological tower (1) are exact (the relative number of mean square departures, with respect to angle, of the measurements of brightness temperature from calculations is based on measured data from RASS or from the meteorological tower).

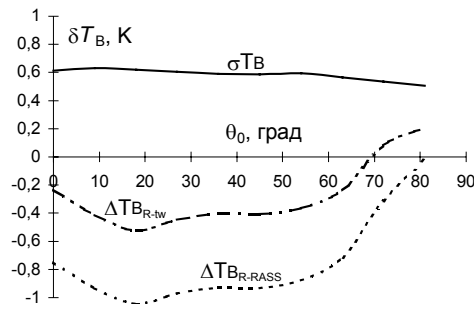


Fig. 1. The errors of radiometric measurements.
 (1) σT_B ; (2) $\Delta T_{B,R-tw}$; (3) $\Delta T_{B,R-RASS}$

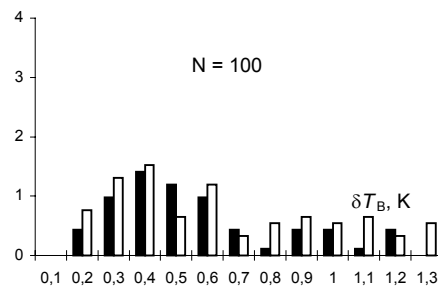


Fig.2. Histogram of the probability density of the distribution of errors of Tikhonov's method for temperature profiles reconstructed from (1) meteorological tower data and (2) RASS data.

The position of the maximum of the probability density distribution of the measurement errors for the tower and to RASS (0.4 K) was found to be close to the value of the standard deviation determined above for Tikhonov's method (0.5 K), but the RASS measurements were different in quality, which was obviously connected with the noise that depends on the wind speed. The higher level of the radiometric measurements errors in comparison with the nominal accuracy (0.04 K), aside from the simplified calibration procedure, may be due to the existing cases of rapid temperature changes and to the errors in the standard temperature sensors caused by radiation. In the calibration method, the output of the sensor was considered exact, although, in the present case, as shown by independent in situ measurements, the error of the sensor (0.1-0.2K) invariably affected the calibration. This systematic error with respect to zenith angle is present in every measurement, but in the ensemble, it appears as random.

The possibility of determining the mean square error in the retrieval of temperature profiles permitted the optimization of the retrieval algorithm. It was found that the optimum choice of error for Tikhonov's method was $\delta = \sigma T_B = 0.4K$. For a smaller value, the accuracy of the solution somewhat increased at $h < 150$ m, but decreased at $h > 150$ m. Conversely, with increasing δ , the accuracy of the solution increased $h > 150$ m, but was reduced in the surface layer. The optimal upper boundary (height) of the layer (h_{max}) in which retrievals are practical (the interval in which we have a solution) is 1.5 km, but in integration with consideration of a model temperature profile should be carried out to a height of 5 km. The optimal initial approximation, in the form of the departure from which a solution is sought, was found to be a linear profile. Below 500 m, this profile corresponds to the exact solution of the linear profile equation (10) using brightness temperature measured at zenith. Above 500 m, the initial approximation profile was assumed to be linear, decreasing with a gradient of 6.5 K/km. The mean square departure of brightness temperatures from those calculated in the first approximation is about 2 K for the maximal value of the

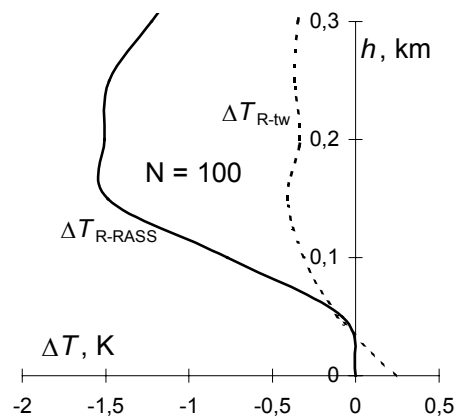
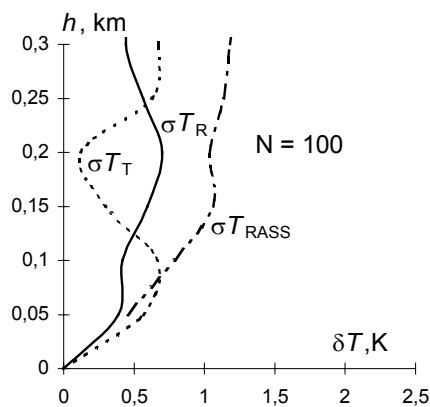


Fig. 3. Root mean square error of three independent methods of temperature determination: (1) radiometric; (2) in situ measurements on meteorological tower, and (3) radioacoustic.

Fig. 4. Difference of systematic errors in the determination of temperature between the radiometric and two other methods: (1) ΔT_{R-tw} ; (2) ΔT_{R-RASS} .

mean square variation of 10 K, which almost exactly corresponds to the temperature variation in the layer 0 – 500 m.

The numerical experiments showed that taking into account the form of the directional diagram improves the retrieval accuracy in the surface layer (0 to 50 m); this, however, cannot be found from available data, because temperature measurements were not taken within this interval.

Simple algorithms of solution were investigated for linear and quadratic temperature profiles. It was found that the method based on the exact solution for a quadratic profile (12) has a large error even for the spline approximation of the measured dependence of the brightness temperature on zenith angle. Its error exceeded 1 K at a height of 100 m.

A simple method based on the exact solution for a linear profile (10) was also tested on the available data. In this case, temperatures obtained from (10) were interpolated by cubic splines in the intervals between levels of the formation of thermal radiation for the corresponding zenith angles. For a relatively moderate accuracy of measurements of brightness temperature, the mean square error of this method was found to be close to the errors of Tikhonov's method. However, it should be noted that this is a result of closeness of the average temperature distribution to the linear profile, because there is a natural advantage of (10) as an exact solution for this case. In the presence of inversions, the systematic error of solution (10) quickly grows, and complex profiles cannot be reconstructed, in principle, with its help. Tikhonov's method has a guaranteed convergence for any distribution.

As already noted, in the case when the assigned error for solution in Tikhonov's method is substantially smaller than the real one, which inevitably occurs in its distribution shown in Fig 2, false features of the solution can appear in the form of large-amplitude departures, which naturally make worse the statistical errors of retrieval. When the error parameter prescribed in Tikhonov's method is increased up to the level that includes the maximal possible departures, the real details in the solution are smoothed and the mean square error of retrieval grows for this reason alone. The effective solution of the problem was found by including the algorithm of control of the rise of large deviations. This algorithm checked a departure from results of the exact solution for the linear profile (10), which automatically did not amplify the errors

of the data provided. If this departure exceeded 0.4K, then solution (10) was used instead of Tikhonov's method. For the prescribed error of Tikhonov's method of 0.4K, this took place approximately in 20% of the cases, but the application of this algorithm allowed the reduction of the mean square retrieval error by a factor of two. Method (10) was applied to the algorithm of solution in those rare cases when the departure or the brightness temperatures from the first approximation, as determined from relation (10), was less than the prescribed level of error (in this case, according to Tikhonov's method, the solution is already found).

Figure 3 presents the basic result of the work, the mean square errors of three independent methods of determining of the temperature up to the height of the tower. It is seen that the radiometric method was found to be most accurate below 130 m and above 250 m. Its root mean square error in the layer 0 to 300 m does not exceed 0.6K. It is also seen, that the error of the in situ sensors on the meteorological tower was substantially larger, and it was basically random, as the curves in Fig. 4 show. This figure shows the difference in systematic errors between the radiometric and the other two methods (as already noted, the third difference is determined from the other two).

The systematic and random errors of the RASS data, as can be seen from Figs. 3 and 4, exceed the errors of the other two methods. We note that the best method (Tikhonov's), from the point of view of minimizing the mean square error, perhaps is not optimal for reconstruction of complex temperature profiles in the atmospheric boundary layer, which must be the subject of further investigation.!

Naturally, the question arises about the accuracy of the evaluation of the mean square errors in the determination of temperature by the three methods from the solution of the system (17). The sampling error of the mean square difference for each of the three terms obeys the χ_n^2 distribution, where $n = N = 300$ is the number of degrees of freedom, equal to the sample size under the assumption of uncorrelated measurement errors. For $N > 30$, this distribution practically does not differ from normal, and for the root mean square temperature deviations, the sampling error is about 0.1 K, which confirms the validity of the basic conclusions of the work.

4. CONCLUSIONS

The statistical analysis of the results of measuring temperature profiles in the atmospheric boundary layer by three independent methods (radiometric, radioacoustic, and in situ sensors) allowed the determination of the root mean square error of each of the methods. The analysis also allowed us to optimize the algorithm for the retrieval of temperature profiles from radiometric measurements, based on Tikhonov's method of the generalized residual by means of minimization of its mean square error. I

The radiometric method was found to be not inferior in accuracy to the direct measurements of air temperature on a meteorological tower. Its root mean square error in the layer 0 to 300 m does not exceed 0.6K. The RASS accuracy was significantly worse, and its working capabilities were seriously limited by weather conditions. The data from the sensors on the meteorological tower had errors comparable with the radiometric method, and they cannot be considered in analysis as completely accurate.

Problems of further development of the radiometric method are (1) the extension of the height range of the retrieval of temperature profiles by including measurements at frequencies lying on the slope of the absorption band of oxygen and (2) the improvement of the retrieval algorithm to take into account the characteristics of the boundary-layer stratification.

REFERENCES

- [1] F.P. Vasiyev, Numerical Methods for Solution of Extremum Problems [in Russian], Nauka, Moscow, 1981.
- [2] K. P. Gaikovich, E. N. Kadyrov, A. S. Kosov, and A.V. Troitskii, "Thermal sounding of the boundary layer of the atmosphere at the center of the absorption line of oxygen", *Izv. Vuzov. Radiophysics*, vol. 35, no.3, 1992.
- [3] K. P. Gaikovich, A. N. Reznik, and R. V. Troitskii, "Radiometric method of determining the subsurface profile of temperature and the depth of freezing soil", *Izv. Vuzov, Radiophysics*, vol. 33, no. 12, 1989.

- [4] K. P. Gaikovich and M. I. Sumin, "The possibility of determining meteorological parameters of the boundary layer of the atmosphere from ultra high frequency radiometric measurements", in: Radiometeorology, Proc. 7th All-Union Conference, Suzdal, 21-24 Oct., 1986 [in Russian], Gidrometeoizdat, Leningrad, 1989.
- [5] A. V. Goncharskii, V. V. Stepanov, A. N. Tikhonov, and A. G. Yagola, Regularization Algorithms and a Priori Information [in Russian], Nauka, Moscow, 1983.
- [6] M. G. Kuznhetzova, V. A. Rassadovskii, and A. V. Troitskii, "Remote sounding of the meteorological parameters of a cloudy atmosphere by radiometric methods", *Izv. Vuzov, Radiophysics*, vol. 22, no. 8, 1979.
- [7] M. I. Sumin and A. V. Troitskii, "On the possibilities of the determination of temperature inversions by ground-based remote sounding of the atmosphere in the absorption band of O₂ $\lambda \sim 5$ mm", *Izv. AN USSR, Atmospheric and Oceanic Physics*, vol. 13, no. 9, 1977.
- [8] A. V. Troitskii, "Remote determination of atmospheric temperature from spectral radiometric measurement in the line $\lambda=0.5$ mm", *Izv. Vuzov, Radiophysics*, vol. 29, no. 8, 1986.
- [9] J. Askne, G. Skoog, E. Winberg, "Test of a ground-based microwave radiometer for atmospheric temperature profiling with meteorological applications," *Int. J. Remote Sensing*, vol.6, no.7, 1985.
- [10] C. Dean, L.M. McMillin, W.B. Sweezy, and E.R. Westwater, "Determination of atmosphere temperature profiles from a statistical combination of ground-based profiler and operational NOAA 6/7 satellite retrievals," *J. Climate and Meteorology*, vol.23, no.5, 1984.
- [11] K.P.Gaikovich, V. D. Gromov, E. N. Kadygrov, A. S. Kosov, and A. V. Troitskii, "Thermal sounding of the atmospheric boundary layer in the oxygen band center at 60 GHz", *IEEE Trans. Geosci. and Remote Sensing*, vol. 31, no.1, 1993.
- [12] K. P. Gaikovich, N. N. Markina, A. P. Naumov, et al., "Investigation of remote sensing possibilities of the power atmosphere in the microwave range and aspects of statistical data use", *Int. J. Remote Sensing*, vol. 4, no.2, 1983.
- [13] Y. Han, V. G. Irisov, E. N. Kadygrov, V. Y. Lenskiy, and E. R. Westwater, "Multi-sensors measurements of boundary layer temperature profiles", Proc.7th Atmosphere Radiation Measurement Science Team Meeting, March 3-7, 1997, San Antonio, Texas, USA.
- [14] Y. Han, V.G. Irisov, E. N. Kadygrov, V.Y. Lenskiy, S. A. Viazankin, and E. R. Westwater, "Remote sensing of boundary layer profiles by scanning 5-mm radiometer and RASS: A comparison experiment", Proc.IGARSS 97, 4-8 August, 1997, Singapore.
- [15] E.R.Westwater, "Ground-based passive probing using the microwave spectrum of oxygen", *Radio Science*, vol. 69D, no.9, 1965.
- [16] E.R.Westwater, "Ground-based Determination of Temperature Profile by microwaves, Thesis of Dissertation, University of Colorado, USA, 1970.

8 June, 1988